JACS
JOURNAL OF THE AMERICAN CHEMICAL SOCIETY
pubs.acs.org/JACS
Article

Hydrogen Bond Interaction Networks in the Mixed Pentamers of Hydrogen Sulfide and Water

Pablo Pinacho, Cristóbal Pérez,* Marcel Stahn, Rizalina T. Saragi, Andreas Hansen, Stefan Grimme, Alberto Lesarri,* and Melanie Schnell*

Cite This: J. Am. Chem. Soc. 2025, 147, 18576−18582

ABSTRACT: The observation of gas-phase water clusters has been instrumental in understanding water aggregation and cooperativity, paving the way for solvation models in the bulk. However, the characterization of hydrogen sulfide self-aggregation is still largely unexplored. Here, we investigate two mixed pentamers of hydrogen sulfide and water to examine the influence of the weaker, dispersion-based and less directional interactions caused by hydrogen sulfide. Unprecedented structural resolution was obtained by combination of jet-cooled broadband rotational spectroscopy and quantum-chemical calculations. Specifically, we compare the 4:1 and 1:4 hydrogen sulfide - water pentamers, offering comparison with the prototype homoclusters. Important structural differences are revealed in the hydrogen sulfide clusters, which reorganize to compensate for the weaker sulfur-centered hydrogen bonds. The noncovalent interactions in the pentamers were rationalized using density functional theory and reduced electronic density calculations. Moreover, a comprehensive many-body decomposition energy analysis revealed significant variations in molecule two- and three-body contributions to the total interaction energy based on the relative proportions of H_2O and H_2S. These findings offer new insights into the distinct cooperative forces in water and hydrogen sulfide clusters. The results will improve our understanding and modeling of sulfur-centered hydrogen bonds, which may be useful across various research fields, including protein folding, molecular aggregation, materials science, and computational benchmarking.

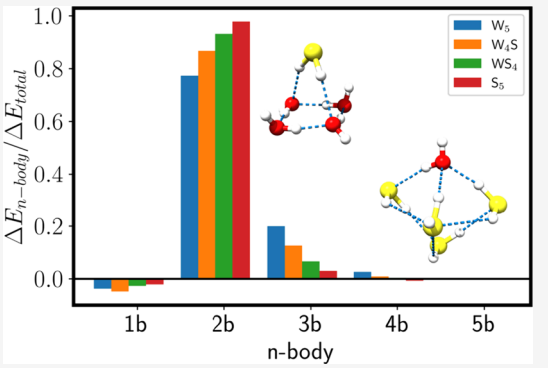

INTRODUCTION

The striking difference between liquid water and gaseous hydrogen sulfide is a textbook example of the relevance of hydrogen bonding. While oxygen and sulfur are isovalent chalcogens, their electronic properties translate into different electronegativities and polarizabilities, resulting in distinctive intermolecular interactions and macroscopic properties of the two dihydrides. Extensive endeavors have been dedicated to study water from a molecular point of view,[1,2] but still no model offers a satisfactory connection between its microscopic molecular properties and the bulk.[3] The most useful molecular strategy is disaggregation by analyzing small size-controlled water clusters in the gas phase at low temperatures, typically in a jet expansion. The combination of high-resolution spectroscopy experiments and quantum-chemical calculations has now progressed from the water dimer[4−7] to the decamers,[8−15] offering detailed pictures on hydrogen bond aggregation patterns,[8−11,13,14] internal dynamics,[10,12] and cooperativity[9,15] that may guide the construction of theoretical models for larger adducts. Among gas-phase techniques, jet-cooled microwave spectroscopy provides detailed structural insights of molecules and complexes, enabling a direct characterization of intermolecular interactions through the moments of inertia, free of solvation or crystal packing effects.[16−18]

Conversely, information on gas-phase hydrogen sulfide aggregates is practically absent, despite sulfur's prevalence and its important chemical role. Hydrogen bonds involving sulfur play an important role in proteins, molecular assemblies and functional materials,[19−21] and their relative strength compared to the oxygen counterparts has been debated.[22−24] Most of the existing gas-phase information concerns the thiol group acting as proton acceptor, as in the O−H···S,[25−28] N−H···S,[29−32] and C−H···S[33,34] hydrogen bonds. However, the observations of thiols as proton donor (S−H···O,[35−37] S−H···N,[38] S−H···π,[39−41] etc.) or the elusive S−H···S hydrogen bond[42−48] are limited to a few cases. The experimental information on hydrogen sulfide aggregates is even more scarce and restricted to the $(H_2S)_2$ dimer,[35,42−44] the $(H_2S)_2$···(H_2O)

Received: January 8, 2025
Revised: May 7, 2025
Accepted: May 19, 2025
Published: May 26, 2025

trimer[49] and several argon complexes (Ar···(H_2S),[50] Ar_2···(H_2S),[51] and Ar_3···(H_2S)[52]). A vibrational study recently reported the observation of the dimer, trimer, and tetramer in a cold argon matrix,[48] but its low resolution makes the rotational investigation of larger hydrogen sulfide clusters a fundamental topic for noncovalent interactions.

The water trimer, tetramer and pentamer feature cyclic near-planar ring geometries of the oxygen atoms and, therefore, are nonpolar and not detectable by rotational spectroscopy.[8−15] However, the potential energy surface (PES) of hydrogen sulfide is more complex. Previous theoretical studies explored the $(H_2S)_n$ complexes up to the pentamer,[53−55] and its mixed clusters with water up to the tetramer,[56] showing that in the presence of hydrogen sulfide three-dimensional structures are preferred over the planar rings in the tetramer and pentamer. The addition of even just one H_2S molecule to the water structures induces a transition from two-dimensional to three-dimensional heavy-atom shapes, enabling their analysis by rotational spectroscopy.

We report here on two water-mixed pentamers of hydrogen sulfide, with the objectives of studying the nature of the sulfur-centered intermolecular interactions, the formation of cooperative hydrogen-bonded networks, the cluster-growth mechanisms, and the differences with the water prototypes. Since computational methods perform worse for the heavier chalcogens compared to oxygen, the experimental studies may serve also as benchmarking references for the tasks of conformational search and structural and energetic determination of their shallow PES.

These mixed clusters offer an exceptional opportunity to observe the molecular effects of introducing a competing chalcogen molecule into the homomeric structures, shedding light on the electronic and structural differences. At the same time, the asymmetry introduced by the different chemical species eliminates tunneling effects arising from large-amplitude motions. This fact reduces the complexity of the spectral analysis and makes them suitable for the investigation of their aggregation properties and benchmarking of computational methods. In addition, the mixed dimers are useful gauges of the relative strength of the intermolecular interactions of hydrogen sulfide and water within a single cluster as well as of the occurrence of cooperative effects.

RESULTS

Rotational Spectra of the Mixed Pentamers. The microwave spectrum of hydrogen sulfide and water in Figure 1 is very complex and congested (roughly 6200 transitions with signal-to-noise ratio above 3:1 in the 2−12 GHz region), containing rotational signatures from multiple clusters of different size and chemical composition. This included, despite having weak intensities, rotational transitions from water clusters up to the heptamer. Some of the most prominent lines, apart from those from the hydrogen sulfide dimer, were soon attributed to pentameric species, suggesting these species for an initial study. In this report, we present the results concerning the (H_2O)-$(H_2S)_4$ and $(H_2O)_4$-(H_2S) mixed pentamers (later abbreviated WS_4 and W_4S, respectively). The pure hydrogen sulfide pentamer could not be assigned because of extensive tunnelling effects hindering the spectral analysis.

Different computational models were used in this study, including B3LYP-D3(BJ)/def2-TZVP,[57−59] ωB97X-V/def2-TZVP,[60] and MP2/aug-cc-pVTZ.[61−63] A complete description

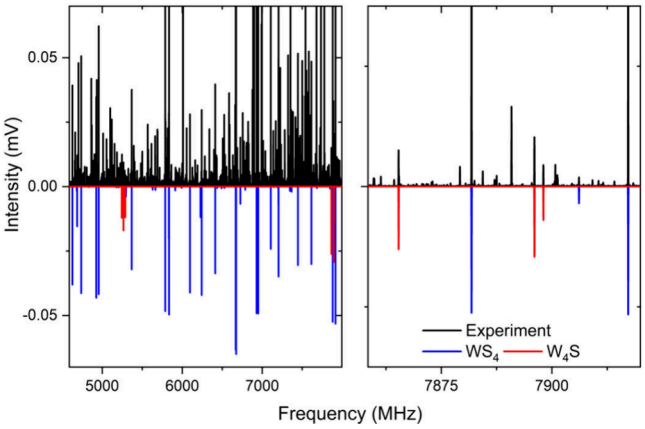

Figure 1. Left panel shows a section of the experimental rotational spectrum of a gas mixture of H_2S and H_2O, highlighting the high density of lines. The right panel shows selected rotational transitions for WS_4 and W_4S clusters in blue and red, respectively. The colored traces are simulations with a rotational temperature of 2 K based on the fitted rotational parameters in Tables 1 and 2.

of the computational methodology and theoretical results is given in the Supporting Information. The conformational search focused on the detection of the global minimum and the lowest energy isomers. For both pentamers W_4S and WS_4, the computational methods predicted three isomers in a narrow energy range below 3 kJ·mol^{-1} (Tables S1−S2, Figure 2).

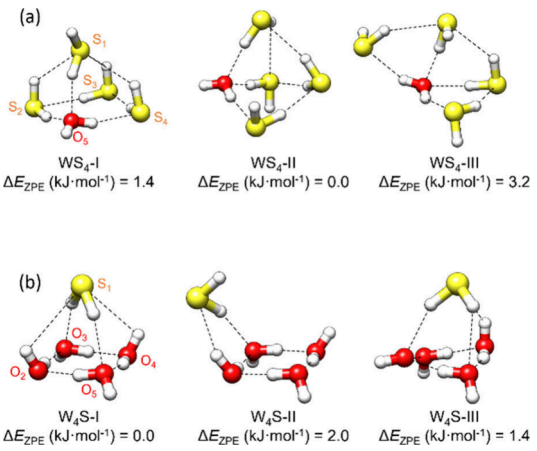

Figure 2. Predicted lowest-energy structures for WS_4 (a) and W_4S (b) (ωB97X-V/def2-TZVP), including the relative electronic energy with zero-point energy correction.

The rotational spectrum was first examined to exclude previously identified species. Once the transitions belonging to the hydrogen sulfide dimer[43] were removed from the spectrum, some intense lines showing characteristic *a*-, *b*-, and *c*-type quartets were first identified. Since the rotational constants critically depend on the cluster size and geometry, the (ground-state) experimental values were compared with the (equilibrium) computational predictions. The experimental transition intensities provided a second discrimination argument (Table 1, Figure S1). Both comparisons showed an excellent agreement with the predictions for the WS_4−I isomer of the mixed pentamer $(H_2O)_1$-$(H_2S)_4$, confirming the detection of this species. The later observation of the ^{34}S isotopologues in natural abundance (4.3%) and the determi-

https://doi.org/10.1021/jacs.4c18276
J. Am. Chem. Soc. 2025, 147, 18576−18582

Table 1. Rotational Parameters for (H_2O)-$(H_2S)_4$, Comparing the Experimental Results with the Three Most Stable Isomers (ωB97X-V/def2-TZVP Level)

	Exp.	WS_4-I	WS_4-II	WS_4-III
A/MHz[a]	865.25110(11)[b]	875	824	1077
B/MHz	657.994990(95)	684	596	516
C/MHz	564.323353(88)	576	585	460
Δ_J/kHz	0.53003(57)	0.33[c]	0.61	0.20
Δ_{JK}/kHz	−1.3627(11)	−0.64	5.34	1.28
Δ_K/kHz	2.9068(12)	1.49	−3.55	−0.30
δ_J/kHz	0.14284(18)	0.09	−0.01	0.01
δ_K/kHz	−0.2598(20)	−0.15	8.60	1.32
μ_a/D	**	1.2	1.5	1.0
μ_b/D	***	3.0	0.8	1.4
μ_c/D	*	0.3	2.4	0.1
N	260	–	–	–
σ/kHz	5.4	–	–	–
ΔE_{ZPE}/kJ·mol^{-1}	–	1.4	0.0	3.2

[a]Rotational constants (A, B, C), quartic centrifugal distortion constants (Δ_J, Δ_{JK}, Δ_K, δ_J, and δ_K), electric dipole-moment components (μ_a, μ_b, and μ_c) and experimental intensities (proportional to the number of asterisks), number of fitted transitions (N), root-mean square deviation of the fit (σ) and relative electronic energy including the zero-point energy correction (ΔE_{ZPE}). [b]Standard errors in parentheses in units of the last digit. [c]The centrifugal distortion constants were computed within the harmonic approximation at the ωB97X-D/def2-TZVP level of theory.

nation of the experimental structure definitively confirmed the assignment.

Due to their small energy difference, isomers WS_4-II and WS_4-III may be populated in the jet, but they were not observed. No large-amplitude motions were observed in the spectrum of WS_4-I, so the spectrum of this isomer could be reproduced with a semirigid rotor model.[64] The fitted rotational parameters (rotational constants and quartic centrifugal distortion constants) are summarized in Table 1.

Further exploration of the spectrum resulted in the fit of a weaker pentamer cluster (in red in Figure 1), producing the rotational parameters given in Table 2. The comparison with the predicted parameters and the observation of only a-type transitions (Table 2, Figure S1) confirmed the identification of the second experimental species as the global minimum of the pentamer $(H_2O)_4$-$(H_2S)_1$, denoted isomer W_4S−I in Figure 2. Some quartic centrifugal distortion constants for this cluster could not be determined because of the reduced number of transitions.

A first comparison of the WS_4 and W_4S isomers is pertinent here. W_4S is characterized by a homodromic water hydrogen-bonded network similar to the pure water tetramer and one out-of-plane sulfur atom. In this geometry, inversion of the water orientation simply produces the enantiomeric species. However, for the lowest energy isomer of WS_4 there are additional degrees of freedom associated to the nonsequential heterodromic hydrogen-bonded network. In consequence, the orientations of the hydrogen atoms generate multiple isomers within the same structural family. However, the slightly different isomers still possess unique rotational constants, dipole-moment components and energies permitting their unequivocal identification (Table S3, Figure S2).

From the three levels of theory employed, the hybrid generalized-gradient-approximation functional ωB97X-V/def2-TZVP gave the best agreement with the experiment, with

Table 2. Rotational Parameters for $(H_2O)_4$-(H_2S), Comparing the Experimental Results with the Three Most Stable Isomers (ωB97X-V/def2-TZVP Level)

	Exp.	W_4S−I	W_4S−II	W_4S−III
A/MHz[a]	1772.37(47)[b]	1823	2571	2042
B/MHz	1327.6340(93)	1410	975	1292
C/MHz	1305.4979(90)	1352	835	1259
Δ_J/kHz	1.547(61)	1.04[c]	1.05	1.28
Δ_{JK}/kHz	48.14(29)	4.87	−3.63	−1.21
Δ_K/kHz	[0]	−5.36	10.82	3.00
δ_J/kHz	[0]	0.05	0.03	−0.07
δ_K/kHz	17.8(45)	3.15	0.56	−5.29
μ_a/D	***	1.1	1.2	2.7
μ_b/D	–	0.0	1.0	2.6
μ_c/D	–	0.0	0.6	0.3
N	16	–	–	–
σ/kHz	6.2	–	–	–
ΔE_{ZPE}/kJ·mol^{-1}	–	0.0	2.0	1.4

[a]Parameter definition as in Table 1. [b]Standard errors in parentheses in units of the last digit. [c]The centrifugal distortion constants were computed within the harmonic approximation at the ωB97X-D/def2-TZVP level of theory.

relative differences in the rotational constants around 4%. The reasons for the better performance compared to higher levels of theory are unclear and could be due to beneficial error cancellation.

Molecular Structure. The structure of the WS_4 pentamer could be assessed using the observations of the four ^{34}S monosubstituted isotopologues (Table S4, Figures S3−S4). This information enabled the determination of the experimental structure, displayed in Figure 3, through the substitution (r_s) and effective (r_0) methods.[65,66] For the determination of the r_0 structure, the monomers were assumed

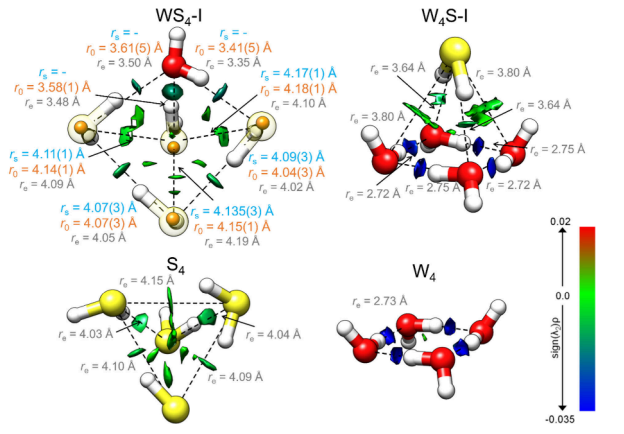

Figure 3. NCI plots[67,68] (isosurface 0.5) for WS_4, W_4S, the hydrogen sulfide (S_4) and the water tetramers (W_4), respectively. The larger spheres are the predicted structures at the ωB97X-V/def2-TZVP level of theory (r_e) along with some intermolecular distances. The smaller, solid spheres overlaid with the structure of WS_4 represent the experimentally determined (r_s) sulfur atom positions obtained from the monoisotopic substitutions in natural abundance. The S···S, S···O, O···S, and O···O distances are given in Å. The strength of the interactions is indicated by the value and sign of the second eigenvalue of the Hessian, λ_2. Negative values indicate a strong attraction and are depicted in blue, while values close to 0 indicate the presence of weak forces and are illustrated in green.

https://doi.org/10.1021/jacs.4c18276
J. Am. Chem. Soc. 2025, 147, 18576−18582

to be unperturbed upon complexation and the distances and angles between the heavy atoms in the cluster were floated, while the rest of the parameters were fixed to their theoretical values at the ωB97X-V/def2-TZVP level. In the r_s structure, the isotopic differences of the moments of inertia are used in the Kraitchman equations to obtain near-equilibrium coordinates. The results of structure determination are reported in detail in the SI (Tables S5−S8).

The WS_4 pentamer features a distorted square pyramid, with the only water molecule positioned in one of the vertices of the base. The four molecules in the base simultaneously act as hydrogen bond donor and acceptor, closing an 8-membered ring. In addition, the three hydrogen sulfide molecules in the base act as proton donors to the molecule in the apex, which is involved in four simultaneous hydrogen-bonding interactions (three as an acceptor and one as donor). In total, one O−H···S, two S−H···O, and five S−H···S individual interactions can be identified. Notably, the S···S interaction previously described as a plausible attractive force[53−56] was not identified in the cluster.

In Figure 3, we compare WS_4 with the homomeric S_4 tetramer obtained from quantum chemistry. It is worth noting that the hydrogen-bonded network present in the pure tetramer closely resembles that identified in WS_4. As depicted, the structure of the pure tetramer is slightly distorted to accommodate the water monomer favorably through the formation of the above-mentioned hydrogen bonding topologies. This does not imply that the formation of this cluster occurs sequentially through the addition of water monomers to the structure of the pure tetramer. Instead, it helps to identify the presence and pervasiveness of specific hydrogen-bonded networks as the cluster complexity increases.

The second pentamer, W_4S, presents a pyramidal shape with a regular square base made of four water units resembling the pure water tetramer (Figure 3). In W_4S, the hydrogen sulfide unit is located in the apex, binding simultaneously to the four water molecules. The inclusion of hydrogen sulfide does not significantly alter the dominant water tetramer but generates a nonplanar structure that maximizes its interactions with water through two O−H···S and two S−H···O hydrogen bonds. The final polyhedric structure reflects the well-known self-aggregation preference of water, whose hydrogen bond is only slightly perturbed to locate the hydrogen sulfide monomer. Overall, both WS_4 and W_4S share the total number of network interactions (eight in total), but of different nature.

A Non-Covalent Interaction (NCI) analysis was performed to visualize the multiple interactions stabilizing the clusters. The plotted surfaces in Figure 3 are based on the reduced density gradient as suggested by Johnson et al.,[67,68] mapping the spatial distribution, attractive character, and strength of the intermolecular forces in the pentamers. This information, together with structural data, confirms the S−H···S hydrogen bond as a weak interaction.

Many-Body Decomposition Energy Analysis. To facilitate the interpretation of our findings and provide a rationale for the structures observed in the clusters, we conducted a comprehensive many-body decomposition (MBD) analysis of the interaction energy for each cluster.[69,70] This analysis yields valuable insights into the strength of specific interactions between molecule pairs, triples, and higher-order groups, as well as their individual contributions to the overall interaction energy. We computed the individual many-body interaction energy components for all monomer sets to isolate each interaction of interest. Additionally, we performed an MBD analysis on the two extreme cases with the same number of monomers, i.e., the pure hydrogen sulfide pentamer (S_5) and the pure water pentamer (W_5), respectively. This allowed us to observe the trend for each *n*-body interaction as the relative number of each type of monomers is reversed. The results of this analysis are illustrated in Figure 4, and the complete set of results is reported in the SI (Table S9 and Figure S5). This analysis was performed at the ωB97X/def2-TZVP level of theory for all 31 possible *n*-body ($n = 1−5$) contributions. Subsequently, we will highlight the most relevant findings.

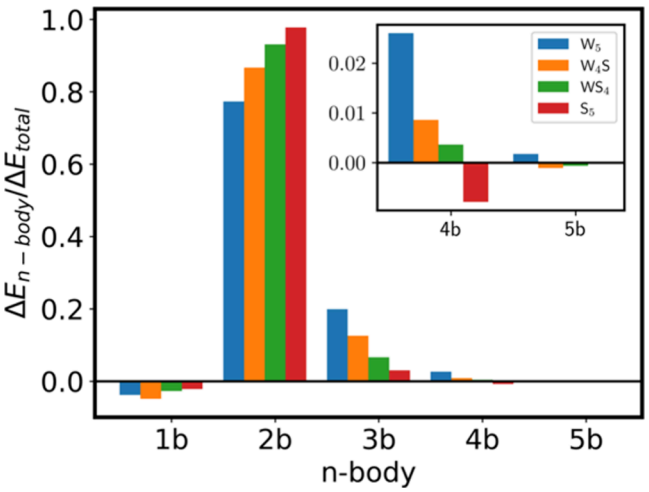

Figure 4. *n*-Body normalized contributions to the total interaction energy for the observed W_4S (orange) and WS_4 (green) clusters compared to the pure water pentamer W_5 (blue) and the pure hydrogen sulfide pentamer S_5 (red). The two- and three-body contributions are the dominant ones and give the clusters their specific structural features. The pairwise contributions increase significantly as the number of H_2S moieties increases. The opposite trend is observed for the three-body interactions. The total interaction/four-body interactions ratio shown in the inset becomes negative for the pure S_5 cluster.

First, we observe that the one-body or deformation energy is in the range of 2−5% of the total energy. This small contribution is expected because the monomers in the cluster are only slightly distorted from their isolated, most stable angular form. Second, the two-body interactions are the main contributors to the global interaction energy, ranging from a 77% for W_5 to a remarkably higher 98% for the pure S_5 cluster. Third, the three-body contributions decrease notably as the amount of H_2S monomers increases in the clusters. In this case, we go from a 20% for W_5 to an almost negligible 3% for S_5.

These results have important implications in the structural features of the observed clusters. In pure water clusters, it is accepted that the three-body interactions are one of the main factors contributing to both the preferred three-dimensional geometries and cooperativity, which remarkably increases the strength of a hydrogen bond as the number of water monomers in the network increases.[71] However, the dramatic decrease in their contribution to the total interaction energy for S_5 clearly indicates that cooperative effects in the aggregation of H_2S are considerably less relevant compared to those in water. What is more, the four-body contributions

https://doi.org/10.1021/jacs.4c18276
J. Am. Chem. Soc. 2025, 147, 18576−18582

become anticooperative for S_5 as shown in the Figure 4 inset. All these findings indicate that the three-dimensional structures are predominantly governed by pairwise interactions, optimizing the geometries of individual dimers, which strongly contributes to the shallow PES observed for clusters containing H_2S and the difficulty encountered for quantum-chemical calculations to explore the structure and energetics of sulfur-centered bonded systems.

CONCLUSIONS

In summary, we used state-of-the-art broadband rotational spectroscopy combined with quantum-chemical calculations to fully characterize the elusive, largely unexplored sulfur-centered hydrogen bonds through the study of two extreme cases of mixed pentamers, i.e., W_4S and WS_4. The high sensitivity and resolution of rotational spectroscopy, together with the exquisite sensitivity to the three-dimensional structure and mass distribution of the clusters under study, enabled us to obtain experimental structural parameters with unprecedented accuracy. In addition, we performed a comprehensive MBD energy analysis of the observed clusters together with pure, homodromic aggregates to gain insight into the individual contributions of particular monomer groups to the total interaction energy. Remarkably, we found that the multibody contributions to the total interaction energy are significantly different as the relative proportions of H_2O−H_2S vary.

These results help to rationalize the observed structures and contribute to a better understanding of the cooperative forces that, while crucial in water clusters, are much less relevant to the global geometry and energetics in H_2S-containing clusters. The current results represent a significant advance in elucidating this underexplored area of sulfur-centered hydrogen bonding. They will undoubtedly contribute to better modeling of these important interactions for a variety of research areas. Future investigations of other hydrogen sulfide adducts may contribute to learn about the internal dynamics of the clusters and to understand how the molecular characteristics contribute to their different macroscopic properties compared to water.

EXPERIMENTAL METHODS

The experimental investigation used broadband microwave spectroscopy in the 2−12 GHz region using the chirped-pulse Fourier transform microwave (CP-FTMW) spectrometer COMPACT.[72] The sample, containing *ca.* 1% of H_2S in neon, was directed to a gas mixing line permitting the addition of water vapor. The complexes were generated by supersonic expansion of the gas mixture (2.5 bar) through a pulsed injection valve (nozzle diameter 1 mm). A short microwave chirped pulse (4 μs) perpendicular to the gas jet produced a transient broadband electric dipole molecular excitation. The resulting free induction decay of the induced macroscopic dipole moment was recorded in a digital oscilloscope (40 μs) and Fourier-transformed to give the frequency spectrum. Typical transitions have full widths at half-maximum of ca. 50 kHz. A complete description of the theoretical and experimental details is given in the Supporting Information. The observed frequencies of the rotational transitions are given in the SI.

ASSOCIATED CONTENT

Supporting Information

The Supporting Information is available free of charge at https://pubs.acs.org/doi/10.1021/jacs.4c18276.

The Supporting Information provides a description of the theoretical and experimental methods, theoretical parameters for the considered structures, experimental data for ^{34}S isotopologues, many-body decomposition analysis energies; and line lists of observed transitions (PDF)

AUTHOR INFORMATION

Corresponding Authors

Cristóbal Pérez − *Deutsches Elektronen-Synchrotron DESY, 22607 Hamburg, Germany; Departamento de Química Física y Química Inorgánica, Facultad de Ciencias − I.U. CINQUIMA, Universidad de Valladolid, 47011 Valladolid, Spain;* orcid.org/0000-0001-5248-5212; Email: cristobal.perez@uva.es

Alberto Lesarri − *Departamento de Química Física y Química Inorgánica, Facultad de Ciencias − I.U. CINQUIMA, Universidad de Valladolid, 47011 Valladolid, Spain;* orcid.org/0000-0002-0646-6341; Email: alberto.lesarri@uva.es

Melanie Schnell − *Deutsches Elektronen-Synchrotron DESY, 22607 Hamburg, Germany; Institut für Physikalische Chemie, Christian-Albrechts-Universität zu Kiel, 24118 Kiel, Germany;* orcid.org/0000-0001-7801-7134; Email: melanie.schnell@desy.de

Authors

Pablo Pinacho − *Deutsches Elektronen-Synchrotron DESY, 22607 Hamburg, Germany; Departamento de Química Física y Química Inorgánica, Facultad de Ciencias − I.U. CINQUIMA, Universidad de Valladolid, 47011 Valladolid, Spain;* orcid.org/0000-0002-6369-4631

Marcel Stahn − *Mulliken Center for Theoretical Chemistry, Institut für Physikalische und Theoretische Chemie, Rheinische Friedrich-Wilhelms-Universität Bonn, 53115 Bonn, Germany;* orcid.org/0000-0003-2567-3917

Rizalina T. Saragi − *Departamento de Química Física y Química Inorgánica, Facultad de Ciencias − I.U. CINQUIMA, Universidad de Valladolid, 47011 Valladolid, Spain; Chemical Sciences and Engineering Division, Argonne National Laboratory, Lemont, Illinois 60439, United States;* orcid.org/0000-0003-4472-357X

Andreas Hansen − *Mulliken Center for Theoretical Chemistry, Institut für Physikalische und Theoretische Chemie, Rheinische Friedrich-Wilhelms-Universität Bonn, 53115 Bonn, Germany;* orcid.org/0000-0003-1659-8206

Stefan Grimme − *Mulliken Center for Theoretical Chemistry, Institut für Physikalische und Theoretische Chemie, Rheinische Friedrich-Wilhelms-Universität Bonn, 53115 Bonn, Germany;* orcid.org/0000-0002-5844-4371

Complete contact information is available at: https://pubs.acs.org/10.1021/jacs.4c18276

Funding

Spanish *Ministerio de Ciencia e Innovación* and the European Regional Development Fund (MICINN − ERDF, Grant No. PID2021−125015NBI00) and the Junta de Castilla y León (Grant INFRARED IR2021-UVa13).

Notes

The authors declare no competing financial interest.

ACKNOWLEDGMENTS

Parts of the computations were performed by using the European XFEL and DESY funded Maxwell computational

resources operated at Deutsches Elektronen-Synchrotron DESY, Hamburg, Germany. Scientific discussions within the framework of the Centre for Molecular Water Science (CMWS) are acknowledged. C.P. thanks Spanish Ministerio de Universidades for the BG20/00160 Beatriz Galindo Senior Researcher at the University of Valladolid, and the ERC for the CoG HydroChiral (Grant Agreement No 101124939)

REFERENCES

(1) Brini, E.; Fennell, C. J.; Fernandez-Serra, M.; Hribar-Lee, B.; Lukšič, M.; Dill, K. A. How Water's Properties Are Encoded in Its Molecular Structure and Energies. *Chem. Rev.* **2017**, *117*, 12385−12414.
(2) Pettersson, L. G. M.; Henchman, R. H.; Nilsson, A. Water—The Most Anomalous Liquid. *Chem. Rev.* **2016**, *116*, 7459−7462.
(3) Cisneros, G. A.; Wikfeldt, K. T.; Ojamäe, L.; Lu, J.; Xu, Y.; Torabifard, H.; Bartók, A. P.; Csányi, G.; Molinero, V.; Paesani, F. Modeling Molecular Interactions in Water: From Pairwise to Many-Body Potential Energy Functions. *Chem. Rev.* **2016**, *116*, 7501−7528.
(4) Dyke, T. R.; Mack, K. M.; Muenter, J. S. The structure of water dimer from molecular beam electric resonance spectroscopy. *J. Chem. Phys.* **1977**, *66*, 498−510.
(5) Keutsch, F. N.; Saykally, R. J. Water clusters: Untangling the mysteries of the liquid, one molecule at a time. *Proc. Natl. Acad. Sci. U.S.A.* **2001**, *98*, 10533−10540.
(6) Harker, H. A.; Keutsch, F. N.; Leforestier, C.; Scribano, Y.; Han, J. X.; Saykally, R. J. Toward a precise determination of the acceptor switching splitting in the water dimer. *Mol. Phys.* **2007**, *105*, 497−512.
(7) Mukhopadhyay, A.; Cole, W. T. S.; Saykally, R. J. The Water Dimer I: Experimental Characterization. *Chem. Phys. Lett.* **2015**, *633*, 13−26.
(8) Keutsch, F. N.; Cruzan, J. D.; Saykally, R. J. The Water Trimer. *Chem. Rev.* **2003**, *103*, 2533−2577.
(9) Cruzan, J. D.; Braly, L. B.; Liu, K.; Brown, M. G.; Loeser, J. G.; Saykally, R. J. Quantifying Hydrogen Bond Cooperativity in Water: VRT Spectroscopy of the Water Tetramer. *Science* **1996**, *271*, 59−62.
(10) Liu, K.; Brown, M. G.; Cruzan, J. D.; Saykally, R. J. Vibration-Rotation Tunneling Spectra of the Water Pentamer: Structure and Dynamics. *Science* **1996**, *271*, 62−64.
(11) Pérez, C.; Muckle, M. T.; Zaleski, D. P.; Seifert, N. A.; Temelso, B.; Shields, G. C.; Kisiel, Z.; Pate, B. H. Structures of cage, prism, and book isomers of water hexamer from broadband rotational spectroscopy. *Science* **2012**, *336*, 897−901.
(12) Richardson, J. O.; Pérez, C.; Lobsiger, S.; Reid, A. A.; Temelso, B.; Shields, G. C.; Kisiel, Z.; Wales, D. J.; Pate, B. H.; Althorpe, S. C. Concerted hydrogen-bond breaking by quantum tunneling in the water hexamer prism. *Science* **2016**, *351*, 1310−1313.
(13) Pérez, C.; Lobsiger, S.; Seifert, N. A.; Zaleski, D. P.; Temelso, B.; Shields, G. C.; Kisiel, Z.; Pate, B. H. Broadband Fourier Transform Rotational Spectroscopy for Structure Determination: The Water Heptamer. *Chem. Phys. Lett.* **2013**, *571*, 1−15.
(14) Pérez, C.; Zaleski, D. P.; Seifert, N. A.; Temelso, B.; Shields, G. C.; Kisiel, Z.; Pate, B. H. Hydrogen bond cooperativity and the three-dimensional structures of water nonamers and decamers. *Angew. Chem., Int. Ed.* **2014**, *53*, 14368−14372.
(15) Xantheas, S. S. Cooperativity and hydrogen bonding network in water clusters. *Chem. Phys.* **2000**, *258*, 225−231.
(16) Grabow, J.-U. Fourier Transform Microwave Spectroscopy Measurement and Instrumentation. In *Handbook of High-Resolution Spectroscopy*; Merkt, F., Quack, M., Eds.; John Wiley & Sons, Ltd: New York, 2011; pp 723−799.
(17) Caminati, W. Microwave Spectroscopy of Large Molecules and Molecular Complexes. In *Handbook of High-Resolution Spectroscopy*; Merkt, F., Quack, M., Eds.; John Wiley & Sons, Ltd: New York, NY, 2011; pp 829−852.
(18) Caminati, W.; Grabow, J.-U. Advancements in Microwave Spectroscopy. In *Frontiers and Advances in Molecular Spectroscopy*; Laane, J., Ed.; Elsevier Inc.: 2018; pp 569−598.
(19) Gregoret, L. M.; Rader, S. D.; Fletterick, R. J.; Cohen, F. E. Hydrogen bonds involving sulfur atoms in proteins. *Proteins: Struct., Funct., Bioinf.* **1991**, *9*, 99−107.
(20) Zhou, P.; Tian, F.; Lv, F.; Shang, Z. Geometric characteristics of hydrogen bonds involving sulfur atoms in proteins. *Proteins: Struct., Funct., Bioinf.* **2009**, *76*, 151−163.
(21) Chand, A.; Sahoo, D. K.; Rana, A.; Jena, S.; Biswal, H. S. The Prodigious Hydrogen Bonds with Sulfur and Selenium in Molecular Assemblies, Structural Biology, and Functional Materials. *Acc. Chem. Res.* **2020**, *53*, 1580−1592.
(22) Biswal, H. S.; Shirhatti, P. R.; Wategaonkar, S. O−H···O versus O−H···S Hydrogen Bonding I: Experimental and Computational Studies on the p-Cresol·H_2O and p-Cresol·H_2S Complexes. *J. Phys. Chem. A* **2009**, *113*, 5633−5643.
(23) Biswal, H. S.; Bhattacharyya, S.; Bhattacherjee, A.; Wategaonkar, S. Nature and strength of sulfur-centred hydrogen bonds: laser spectroscopic investigations in the gas phase and quantum-chemical calculations. *Int. Rev. Phys. Chem.* **2015**, *34*, 99−160.
(24) Biswal, H. S.; Wategaonkar, S. Sulfur, Not Too Far Behind O, N, and C: SH···π Hydrogen Bond. *J. Phys. Chem. A* **2009**, *113*, 12774−12782.
(25) Bhattacharyya, S.; Wategaonkar, S. ZEKE Photoelectron Spectroscopy of p-Fluorophenol···H_2S/H_2O Complexes and Dissociation Energy Measurement Using the Birge−Sponer Extrapolation Method. *J. Phys. Chem. A* **2014**, *118*, 9386−9396.
(26) Ghosh, S.; Bhattacharyya, S.; Wategaonkar, S. Dissociation Energies of Sulfur-Centered Hydrogen-Bonded Complexes. *J. Phys. Chem. A* **2015**, *119*, 10863−10870.
(27) Juanes, M.; Lesarri, A.; Pinacho, R.; Charro, E.; Rubio, J. E.; Enríquez, L.; Jaraíz, M. Sulfur Hydrogen Bonding in Isolated Monohydrates: Furfuryl Mercaptan versus Furfuryl Alcohol. *Chem. − Eur. J.* **2018**, *24*, 6564−6571.
(28) Juanes, M.; Saragi, R. T.; Pinacho, R.; Rubio, J. E.; Lesarri, A. Sulfur hydrogen bonding and internal dynamics in the monohydrates of thenyl mercaptan and thenyl alcohol. *Phys. Chem. Chem. Phys.* **2020**, *22*, 12412−12421.
(29) Biswal, H. S.; Wategaonkar, S. Nature of the N−H···S Hydrogen Bond. *J. Phys. Chem. A* **2009**, *113*, 12763−12773.
(30) Liu, X.; Xu, Y. Infrared and microwave spectra of the acetylene−ammonia and carbonyl sulfide−ammonia complexes: a comparative study of a weak C−H···N hydrogen bond and an S···N bond. *Phys. Chem. Chem. Phys.* **2011**, *13*, 14235−14242.
(31) Biswal, H. S.; Gloaguen, E.; Loquais, Y.; Tardivel, B.; Mons, M. Strength of NH···S hydrogen bonds in methionine residues revealed by gas-phase IR/UV spectroscopy. *J. Phys. Chem. Lett.* **2012**, *3*, 755−759.
(32) Wategaonkar, S.; Bhattacherjee, A. N−H···S Interaction Continues To Be an Enigma: Experimental and Computational Investigations of Hydrogen-Bonded Complexes of Benzimidazole with Thioethers. *J. Phys. Chem. A* **2018**, *122*, 4313−4321.
(33) Cocinero, E. J.; Sánchez, R.; Blanco, S.; Lesarri, A.; López, J. C.; Alonso, J. L. Weak hydrogen bonds C−H···S and C−H···F−C in the thiirane−trifluoromethane dimer. *Chem. Phys. Lett.* **2005**, *402*, 4−10.
(34) Ghosh, S.; Chopra, P.; Wategaonkar, S. C−H···S interaction exhibits all the characteristics of conventional hydrogen bonds. *Phys. Chem. Chem. Phys.* **2020**, *22*, 17482−17493.
(35) Bhattacherjee, A.; Matsuda, Y.; Fujii, A.; Wategaonkar, S. The Intermolecular S−H···Y (Y = S, O) Hydrogen Bond in the H_2S Dimer and the H_2S−MeOH Complex. *ChemPhysChem* **2013**, *14*, 905−914.
(36) Lobo, I. A.; Robertson, P. A.; Villani, L.; Wilson, D. J. D.; Robertson, E. G. Thiols as Hydrogen Bond Acceptors and Donors: Spectroscopy of 2-Phenylethanethiol Complexes. *J. Phys. Chem. A* **2018**, *122*, 7171−7180.
(37) Osseiran, N.; Neeman, E. M.; Dréan, P.; Goubet, M.; Huet, T. R. Insights into the non-covalent interactions of hydrogen sulfide with fenchol and fenchone from a gas-phase rotational study. *Phys. Chem. Chem. Phys.* **2022**, *24*, 24007−24011.

https://doi.org/10.1021/jacs.4c18276
J. Am. Chem. Soc. 2025, 147, 18576−18582

(38) Tubergen, M. J.; Flad, J. E.; Del Bene, J. E. Microwave spectroscopic and ab initio studies of the hydrogen-bonded trimethylamine−hydrogen sulfide complex. *J. Chem. Phys.* **1997**, *107*, 2227−2231.
(39) Arunan, E.; Emilsson, T.; Gutowsky, H. S.; Fraser, G. T.; de Oliveira, G.; Dykstra, C. E. Rotational spectrum of the weakly bonded C_6H_6−H_2S dimer and comparisons to C_6H_6−H_2O dimer. *J. Chem. Phys.* **2002**, *117*, 9766−9776.
(40) Wang, D.; Chopra, P.; Wategaonkar, S.; Fujii, A. Electronic and Infrared Spectroscopy of Benzene-$(H_2S)_n$ (n = 1 and 2): The Prototype of the SH-π Interaction. *J. Phys. Chem. A* **2019**, *123*, 7255−7260.
(41) Jin, Y.; Li, W.; Saragi, R. T.; Juanes, M.; Pérez, C.; Lesarri, A.; Feng, G. Sulfur−arene interactions: the S···π and S−H···π interactions in the dimers of benzofuran···sulfur dioxide and benzofuran··· hydrogen sulfide. *Phys. Chem. Chem. Phys.* **2023**, *25*, 12174−12181.
(42) Lovas, F. J.; Suenram, R. D.; Coudert, L. H. Rotational Spectra and Structures of the H_2S-H_2O and $(H_2S)_2$ Complexes. *43rd International Symposium on Molecular Spectroscopy*; Ohio State University, Columbus, OH (USA), 1988; Comm. RE2.
(43) Das, A.; Mandal, P. K.; Lovas, F. J.; Medcraft, C.; Walker, N. R.; Arunan, E. The H_2S Dimer is Hydrogen-Bonded: Direct Confirmation from Microwave Spectroscopy. *Angew. Chem., Int. Ed.* **2018**, *57*, 15199−15203.
(44) Jäger, S.; Khatri, J.; Meyer, P.; Henkel, S.; Schwaab, G.; Nandi, A.; Pandey, P.; Barlow, K. R.; Perkins, M. A.; Tschumper, G. S.; Bowman, J. M.; van der Avoird, A.; Havenith, M. On the nature of hydrogen bonding in the H_2S dimer. *Nat. Commun.* **2024**, *15*, 9540.
(45) Mishra, K. K.; Borish, K.; Singh, G.; Panwaria, P.; Metya, S.; Madhusudhan, M. S.; Das, A. Observation of an unusually large IR red-shift in an unconventional S−H···S hydrogen-bond. *J. Phys. Chem. Lett.* **2021**, *12*, 1228−1235.
(46) Saragi, R. T.; Juanes, M.; Pérez, C.; Pinacho, P.; Tikhonov, D. S.; Caminati, W.; Schnell, M.; Lesarri, A. Switching hydrogen bonding to π-stacking: The thiophenol dimer and trimer. *J. Phys. Chem. Lett.* **2021**, *12*, 1367−1373.
(47) Saragi, R. T.; Juanes, M.; Pinacho, R.; Rubio, J. E.; Fernández, J. A.; Lesarri, A. Molecular Recognition, Transient Chirality and Sulfur Hydrogen Bonding in the Benzyl Mercaptan Dimer. *Symmetry (Basel)* **2021**, *13*, 2022.
(48) Monu; Oram, B. K.; Bandyopadhyay, B. Revisiting the IR Spectra of H_2S in an Argon Matrix: Identification of $(H_2S)_n$ ($n \leq 4$) Clusters via the Spectral Assignment of ν_{S-H} Transitions. *J. Phys. Chem. A* **2024**, *128*, 6703−6713.
(49) Das, A.; Gougoula, E.; Walker, N.; Arunan, E. Structure and Dynamics of the Weakly Bound $(H_2S)_2(H_2O)$ Observed Using Rotational Spectroscopy. *75th International Symposium on Molecular Spectroscopy*, University of Illinois at Urbana-Champaign: Urbana-Champaign, IL (USA), **2022**, Comm. FA07.
(50) Gutowsky, H. S.; Emilsson, T.; Arunan, E. Rotational spectra, structure, and internal dynamics of Ar−H_2S isotopomers. *J. Chem. Phys.* **1997**, *106*, 5309−5315.
(51) Mandal, P. K.; Ramdass, D. J.; Arunan, E. Rotational spectra and structure of the Ar_2−H_2S complex: pulsed nozzle Fourier transform microwave spectroscopic and ab initio studies. *Phys. Chem. Chem. Phys.* **2005**, *7*, 2740.
(52) Arunan, E.; Emilsson, T.; Gutowsky, H. S.; Dykstra, C. E. Rotational spectra and structures of the Ar_3−H_2O and Ar_3−H_2S symmetric tops. *J. Chem. Phys.* **2001**, *114*, 1242−1248.
(53) Ibargüen, C.; Guerra, D.; Hadad, C. Z.; Restrepo, A. Very weak interactions: structures, energies and bonding in the tetramers and pentamers of hydrogen sulfide. *RSC Adv.* **2014**, *4*, 58217−58225.
(54) Sarkar, S.; Monu, M.; Bandyopadhyay, B. Cooperative nature of the sulfur centered hydrogen bond: investigation of $(H_2S)_n$ (n = 2−4) clusters using an affordable yet accurate level of theory. *Phys. Chem. Chem. Phys.* **2019**, *21*, 25439−25448.
(55) Monu; Oram, B. K.; Bandyopadhyay, B. A unified cost-effective method for the construction of reliable potential energy surfaces for H_2S and H_2O clusters. *Phys. Chem. Chem. Phys.* **2021**, *23*, 18044−18057.
(56) Monu; Kumar Oram, B.; Bandyopadhyay, B. Bridging H_2O and H_2S homomeric clusters via H_2O-H_2S mixed clusters: Impact of the changing ratio of H_2O and H_2S moieties. *Comput. Theor. Chem.* **2022**, *1213*, 113740.
(57) (a) Lee, C.; Yang, W.; Parr, R. G. Development of the Colle-Salvetti correlation-energy formula into a functional of the electron density. *Phys. Rev. B* **1988**, *37*, 785−789. (b) Becke, A. D. Density-functional thermochemistry. III. The role of exact exchange. *J. Chem. Phys.* **1993**, *98*, 5648−5652. (c) Vosko, S. H.; Wilk, L.; Nusair, M. Accurate spin-dependent electron liquid correlation energies for local spin density calculations: a critical analysis. *Can. J. Phys.* **1980**, *58*, 1200−1211.
(58) Grimme, S.; Antony, J.; Ehrlich, S.; Krieg, H. A consistent and accurate ab initio parametrization of density functional dispersion correction (DFT-D) for the 94 elements H-Pu. *J. Chem. Phys.* **2010**, *132*, 154104.
(59) (a) Weigend, F.; Ahlrichs, R. Balanced basis sets of split valence, triple zeta valence and quadruple zeta valence quality for H to Rn: Design and assessment of accuracy. *Phys. Chem. Chem. Phys.* **2005**, *7*, 3297−3305. (b) Weigend, F. Accurate Coulomb-fitting basis sets for H to Rn. *Phys. Chem. Chem. Phys.* **2006**, *8*, 1057−1065.
(60) Mardirossian, N.; Head-Gordon, M. ωB97X-V: A 10-parameter, range-separated hybrid, generalized gradient approximation density functional with nonlocal correlation, designed by a survival-of-the-fittest strategy. *Phys. Chem. Chem. Phys.* **2014**, *16*, 9904−9924.
(61) Møller, C.; Plesset, M. S. Note on an Approximation Treatment for Many-Electron Systems. *Phys. Rev.* **1934**, *46*, 618−622.
(62) Kendall, R. A.; Dunning, T. H.; Harrison, R. J. Electron affinities of the first-row atoms revisited. Systematic basis sets and wave functions. *J. Chem. Phys.* **1992**, *96*, 6796−6806.
(63) Woon, D. E.; Dunning, T. H. Gaussian basis sets for use in correlated molecular calculations. III. The atoms aluminum through argon. *J. Chem. Phys.* **1993**, *98*, 1358−1371.
(64) Watson, J. K. G. In *Vibrational Spectra and Structure, Vol. 6*; Durig, J. R., Ed.; Elsevier B.V.: Amsterdam, 1977; pp 1−89.
(65) Kraitchman, J. Determination of Molecular Structure from Microwave Spectroscopic Data. *Am. J. Phys.* **1953**, *21*, 17−24.
(66) Rudolph, H. D.; Demaison, J. Determination of the Structural Parameters from the Inertial Moments. In *Equilibrium Molecular Structures*; Demaison, J., Boggs, J. E., Csaszar, A. G., Eds.: CRC Press: Boca Raton, FL, 2011; pp 125−158.
(67) Johnson, E. R.; Keinan, S.; Mori-Sánchez, P.; Contreras-García, J.; Cohen, A. J.; Yang, W. Revealing Noncovalent Interactions. *J. Am. Chem. Soc.* **2010**, *132*, 6498−6506.
(68) Contreras-García, J.; Johnson, E. R.; Keinan, S.; Chaudret, R.; Piquemal, J. P.; Beratan, D. N.; Yang, W. NCIPLOT: a program for plotting non-covalent interaction regions. *J. Chem. Theory Comput.* **2011**, *7*, 625−632.
(69) Richard, R. M.; Herbert, J. M. A generalized many-body expansion and a unified view of fragment-based methods in electronic structure theory. *J. Chem. Phys.* **2012**, *137*, 064113.
(70) Steber, A. L.; Temelso, B.; Kisiel, Z.; Schnell, M.; Pérez, C. Rotational dive into the water clusters on a simple sugar substrate. *Proc. Natl. Acad. Sci. U.S.A.* **2023**, *120*, e2214970120.
(71) Tainter, C. J.; Skinner, J. L. The water hexamer: Three-body interactions, structures, energetics, and OH-stretch spectroscopy at finite temperature. *J. Chem. Phys.* **2012**, *137*, 104304.
(72) Schmitz, D.; Alvin Shubert, V.; Betz, T.; Schnell, M. Multi-resonance effects within a single chirp in broadband rotational spectroscopy: The rapid adiabatic passage regime for benzonitrile. *J. Mol. Spectrosc.* **2012**, *280*, 77−84.

https://doi.org/10.1021/jacs.4c18276
J. Am. Chem. Soc. 2025, 147, 18576−18582